Colloidal RuB/Al$_2$O$_3$·xH$_2$O catalyst for liquid phase hydrogenation of benzene to cyclohexene

Jianqiang Wang[a], Pingjun Guo[a], Shirun Yan[a],
Minghua Qiao[a,*], Hexing Li[b], Kangnian Fan[a,*]

[a] Department of Chemistry and Shanghai Key Laboratory of Molecular Catalysis and Innovative Materials,
Fudan University, No. 220 Handan Road, Shanghai 200433, PR China
[b] Department of Chemistry, Shanghai Normal University, Shanghai 200234, PR China

Abstract

A colloidal RuB/Al$_2$O$_3$·xH$_2$O catalyst has been synthesized through a combined coprecipitation–crystallization–reduction strategy and characterized in detail with techniques including ICP-AES, N$_2$ physisorption, XRD, TG/DTA, PSD and TEM. The catalytic behavior in liquid phase selective hydrogenation of benzene to cyclohexene was studied and compared with that of the RuB/γ-Al$_2$O$_3$ catalyst prepared by the incipient-wetness impregnation method. The RuB/Al$_2$O$_3$·xH$_2$O catalyst is found more reactive than the RuB/γ-Al$_2$O$_3$ catalyst, and the maximum yield of cyclohexene is about four times as high as that over the latter. The better activity of the colloidal catalyst is assigned to the higher dispersion of the smaller RuB particles, whereas its superior selectivity is attributed to the improved hydrophilicity due to higher content of structural water and surface hydroxyl groups.
© 2004 Elsevier B.V. All rights reserved.

Keywords: Benzene; Cyclohexene; Hydrogenation; Ruthenium; Aluminum hydroxide; Alumina; Hydrophilicity

1. Introduction

Cyclohexene and its derivatives are important intermediates for chemical industry. Thus the preparation of cyclohexene has triggered great research interest academically and industrially [1–4]. Among various synthetic routes, selective hydrogenation of benzene to cyclohexene is the most promising one, considering the low price of the raw material, the simplicity of the process, along with the atomically economical character of the reaction [5].

Based on numerous research works, it has been acknowledged that ruthenium is the most suitable metal for this reaction, especially when it is aided with zinc sulfate [5–7] or

alkali [8,9]. On the other hand, water is found crucial for a high yield of cyclohexene. Struijk et al. proposed that water might adsorb on the catalyst surface and form a thin stagnant layer which can retard the readsorption of the formed cyclohexene on the catalyst [10]. This speculation is corroborated by the experimental facts that the hydrophilicity of the support is closely related with the yield of cyclohexene. Nagahara and Konishi observed that Ru supported on hydrophilic SiO$_2$ and Al$_2$O$_3$ exhibited better selectivity than that on hydrophobic active carbon [11]. Similarly, Hronec et al. found that the selectivity to cyclohexene over Ru catalyst supported on a strongly hydrophilic potassium methacryloyl ethylene sulfphonate resin is much higher than that displayed by Ru supported on charcoal [12].

In the last two decades, metal boride catalysts derived from reduction of metal salts with borohydride, bearing the nanosize and amorphous structure, have been regarded promising

* Corresponding authors. Tel.: +86 21 65643977; fax: +86 21 65642978.
E-mail addresses: mhqiao@fudan.edu.cn (M. Qiao),
knfan@fudan.edu.cn (K. Fan).

for a variety of catalytic processes [13–16]. We have previously prepared ultrafine RuB powders [17], RuB/SiO$_2$ [18] and RuB/ZrO$_2$·xH$_2$O [19] for benzene selective hydrogenation, with high selectivity to cyclohexene being achieved. It is noted that although the boron contents in the Ru-Zn, the Ru-Zn/SiO$_2$ and the Ru/binary oxides catalysts prepared by reduction with metal borohydride [9,20,21], were not specified, such catalysts virtually belong to this category. On the other hand, although several Ru/Al$_2$O$_3$ catalysts have been employed in benzene selective hydrogenation, they always afforded a cyclohexene yield lower than 30 mol% [4,5,22,23]. Such catalysts were mainly prepared by incipient-wetness impregnation [4,5] or by chemical mixing [22,23], and reduced by hydrogen. Ruthenium boride supported on Al$_2$O$_3$ or Al$_2$O$_3$-related materials, however, has not been tested in this reaction so far.

In the present work, we prepared a colloidal RuB/Al$_2$O$_3$ ·xH$_2$O catalyst through a combined coprecipitation–crystallization–reduction method with the aim of improving the hydrophilicity of the catalyst and consequently the selectivity to cyclohexene. The properties of the catalyst were characterized by inductively coupled plasma-atomic emission spectroscopy (ICP-AES), nitrogen physisorption, powder X-ray diffraction (XRD), thermogravimetric/differential thermal analysis (TG/DTA), particle size distribution (PSD) and transmission electron spectroscopy (TEM). It has been found that such a strategy really works, the cyclohexene yield being about four times as high as that over the RuB/γ-Al$_2$O$_3$ catalyst prepared by the impregnation method.

2. Experimental

2.1. Catalyst preparation

In a typical procedure, 40 ml of 3.0 M ammonia was added dropwise within 40 min through a peristaltic pump to 170 ml of mixed aqueous solution of ruthenium trichloride (2.33 × 10^{-3} M) and aluminum nitrate (0.12 M) thermostated at 323 K under vigorous stirring. After addition, the agitation was maintained for another 40 min for complete hydrolysis. The precipitate was aged in the mother liquor overnight at room temperature before being washed with deionized water to neutrality. The aged precipitate, together with 100 ml of deionized water, was injected to an autoclave for crystallization under autogenous pressure at 453 K for 2 h to obtain the catalyst precursor. Then the catalyst precursor including water was transferred into a three-necked flask thermostated at 288 K, and reduced by 10 ml of KBH$_4$ aqueous solution (0.39 M). The molar ratio of KBH$_4$/Ru was 10/1 to ensure the complete reduction of ruthenium. During the reduction, high purity nitrogen was introduced into the flask as a shelter gas. The as-produced RuB/Al$_2$O$_3$·xH$_2$O catalyst was washed with deionized water at least three times before characterization and activity tests. As the RuB/Al$_2$O$_3$·xH$_2$O catalyst prepared in this way is colloidal, its weight is ex-

pressed by the theoretic amount of Al$_2$O$_3$ and RuB in the catalyst.

The RuB/γ-Al$_2$O$_3$ catalyst was prepared by the incipient-wetness impregnation method. One gram of pre-dried γ-Al$_2$O$_3$ (40–60 mesh, 152.2 m^2 g^{-1}) was impregnated with 2.0 ml of 0.20 M RuCl$_3$ aqueous solution. After being dried at 383 K overnight, the precursor was reduced by the same amount of KBH$_4$ and washed in the same way as described above. Both catalysts have the same nominal Ru loading of 4.0 wt.%.

2.2. Characterization

The compositions of the RuB catalysts were determined by ICP-AES (Thermal Elemental IRIS Intrepid).

The BET surface area, pore volume and average pore diameter of the RuB/γ-Al$_2$O$_3$ catalyst were measured on a Micromeritics TriStar3000 adsorption apparatus by N$_2$ physisorption at 77 K. Catalyst with the storage liquid was transferred to the adsorption glass tube and heated at 383 K under ultrapure nitrogen flow for 2.0 h before measurement. It was weighed by difference in the adsorption tube on completion of the experiment. Since the RuB/Al$_2$O$_3$·xH$_2$O catalyst is colloidal, no attempt was made to acquire its textural property by N$_2$ physisorption.

XRD patterns were collected on a Bruker AXS D8 Advance X-ray diffractometer using Cu Kα radiation (λ = 0.15418 nm). The tube voltage and current were 40 kV and 40 mA, respectively. Catalyst with solvent was placed on the sample stage, with argon flow (99.9995%) purging the sample during the detection to avoid oxidation.

TG and DTA were performed on a Perkin Elmer DTA-7/TGA-7 instrument under an ultrapure nitrogen flow of 50 cm^3 min^{-1}. The sample temperature was raised from 300 to 800 K at a heating rate of 10 K min^{-1}. The Pt crucible was used as the sample holder and the reference compound in DTA measurement was α-Al$_2$O$_3$.

Particle size analysis of the RuB/Al$_2$O$_3$·xH$_2$O catalyst was conducted on a Horiba LB-500 analyzer, which can measure from nano- to micro-dimensions with precision using the dynamic light scattering method. Particle refractive index was set as 1.57 using the main component of Al(OH)$_3$.

The morphology of the as-prepared catalysts and the size of the RuB particles were observed by TEM (JEOL JEM2011) fitted with an energy dispersive X-ray emission analyzer (EDX) which made it possible to identify the distribution of RuB. An accelerating voltage of 200 kV was used for TEM detection. The amorphous character of RuB was verified by selected-area electron diffraction (SAED).

2.3. Activity evaluation and product analysis

About 1 g of the as-prepared catalyst, 50 ml of benzene, 100 ml of water, and an appropriate amount of additive, ZnSO$_4$·7H$_2$O, were added into a 500 ml stainless steel autoclave equipped with a mechanical stirrer. The autoclave

Table 1
The physico-chemical characters of the RuB/Al$_2$O$_3$·xH$_2$O and RuB/γ-Al$_2$O$_3$ catalysts

Catalyst	Composition (atomic ratio)	S_{BET} (m^2 g^{-1})	V_{pore} (cm^3 g^{-1})	d_{pore} (nm)	d_{Ru}[a] (nm)
RuB/Al$_2$O$_3$·xH$_2$O	Ru$_{35.5}$B$_{64.5}$	–	–	–	3.6
γ-Al$_2$O$_3$	–	152.2	0.49	13.0	–
RuB/γ-Al$_2$O$_3$	Ru$_{30.6}$B$_{69.4}$	152.4	0.45	11.7	10

[a] Measured by TEM.

was sealed and the air was flushed out by low pressure H$_2$ several times. The hydrogenation reaction was carried out at temperature of 418 K, hydrogen pressure of 4.28 MPa, and a stirring rate of 1000 rpm. Preliminary tests carried out with different amount of catalysts (0.5–1.0 g) and stirring rates (500–1000 rpm) indicated that the conditions employed in the present reactions had eliminated the gas–liquid mass-transfer limitations. The reaction mixture was sampled at intervals and analyzed chromatographically employing the PEG-20M capillary column and the TCD detector. Under the present reaction conditions, no products other than cyclohexene and cyclohexane were detected during the hydrogenation process.

3. Results and discussion

3.1. Characterization

The chemical compositions of the RuB alloy in the RuB/Al$_2$O$_3$·xH$_2$O and RuB/γ-Al$_2$O$_3$ catalysts are listed in Table 1. For the RuB/Al$_2$O$_3$·xH$_2$O catalyst, the bulk composition is found to be Ru$_{35.5}$B$_{64.5}$ in the atomic ratio, while for the RuB/γ-Al$_2$O$_3$ catalyst the B content is increased to 69.4 mol%. When studying the effect of pH on the composition of the NiB alloy, He et al. found that the higher the pH of the Ni^{2+} solution, the higher is the boron content in the resulting alloy [24], which is in agreement with the mechanism when borohydride is used as the reductant [25]. In the present case, since the volume of the colloidal precursor is much larger than that of RuCl$_3$/γ-Al$_2$O$_3$, upon addition of the basic KBH$_4$ solution, the pH of the former is expected to be lower than that of the latter due to the dilution effect, thus leading to a higher B content. Also listed in Table 1 are the BET surface area, pore volume and pore size of the RuB/γ-Al$_2$O$_3$ catalyst and original γ-Al$_2$O$_3$. The virtually unchanged BET surface area ($\sim$152 m^2 g^{-1}) and the slight drop in pore volume and pore size indicate that the RuB particles were highly dispersed on the support and no obvious blockage of the pores occurred.

Fig. 1 is the XRD profiles of the RuB/γ-Al$_2$O$_3$ and RuB/Al$_2$O$_3$·xH$_2$O catalysts. It is found that the diffraction pattern of the RuB/γ-Al$_2$O$_3$ catalyst is very similar to that of γ-Al$_2$O$_3$ [26] as labeled in Fig. 1, except for a weak but broad peak at 2θ of 43.1° attributable to RuB of amorphous character [18].

The diffraction pattern of the RuB/Al$_2$O$_3$·xH$_2$O catalyst is more complicated. In Fig. 1, besides the features due to bayerite (α-Al(OH)$_3$, JCPDS #20-11) and gibbsite

(γ-Al(OH)$_3$, JCPDS #33-18), there are diffraction peaks at 2θ of 14.4°, 27.9°, 38.2°, 44.3°, 49.2° and 70.7°, which can be assigned either to boehmite or to pseudoboehmite (AlOOH) if only based on the peak position [26]. The subtle difference between pseudoboehmite and boehmite has been investigated by many groups and it is accepted that boehmite and pseudoboehmite represent essentially the same phase with the former having well defined large crystals and lower water content [27–29]. Thus, the XRD pattern of pseudoboehmite exhibits widened lines that coincide in position with boehmite. Based on those works and the relatively broad peak width in the present case, we attribute these six diffraction peaks to pseudoboehmite rather than boehmite.

The formation of pseudoboehmite is further verified by the endothermic peak at 734 K in the DTA curve for the RuB/Al$_2$O$_3$·xH$_2$O catalyst, as shown in Fig. 2a. According to previous works [28,30–32], the crystal transformation temperature of pseudoboehmite to transitional alumina is about 730 K, while the transformation of boehmite to transitional alumina occurs at $\sim$770 K, which is due to the difference in the hydrogen-bond strength between double layers. In addition, the existence of bayerite is confirmed by a single endothermic peak at 591 K, responsible for the decomposition of bayerite to η-Al$_2$O$_3$ [33].

Besides the above two endothermic peaks, the RuB/Al$_2$O$_3$·xH$_2$O catalyst exhibits three peaks at around 370, 466 and 560 K, respectively. The first low temperature peak can be readily ascribed to the desorption of loosely bound physisorbed water. The second endothermic peak
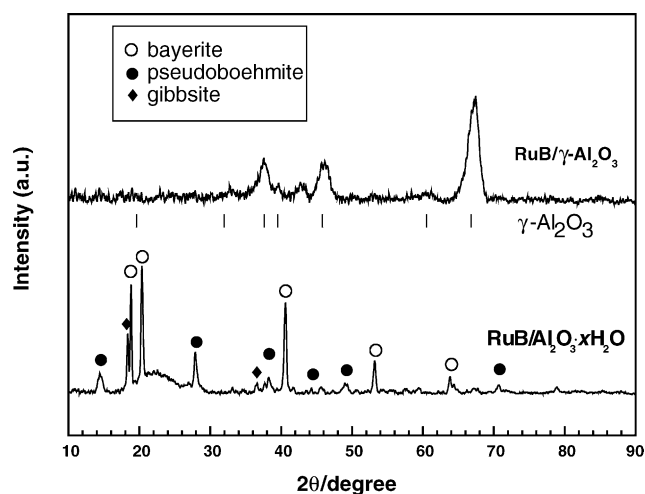

Fig. 1. The XRD patterns of the RuB/Al$_2$O$_3$·xH$_2$O and RuB/γ-Al$_2$O$_3$ catalysts. The tick marks are indicated for γ-Al$_2$O$_3$.

centered at ~466 K represents strongly bound water associated with the amorphous structure of aluminum hydroxide [34], suggesting that a trace amount of amorphous aluminum hydroxide still remains in the sample after the crystallization treatment. On the other hand, Morgado et al. also observed the exothermic peak at around 560 K and assigned it to water loss from structural hydroxyl groups [34]. In agreement with these DTA peaks, the TG curve of the RuB/$Al_2O_3 \cdot x$H$_2$O catalyst exhibits stepwise weight loss, further corroborating the above assignments. It should be noted that from the DTA curve of the RuB/$Al_2O_3 \cdot x$H$_2$O catalyst we cannot obtain any definite information about gibbsite, indicating its negligible amount in the catalyst.

Fig. 2b displays the DTA and TG curves of the RuB/γ-Al_2O_3 catalyst. Different to the RuB/$Al_2O_3 \cdot x$H$_2$O catalyst, the RuB/γ-Al_2O_3 catalyst has only a single endothermic peak centered at 367 K and a corresponding weight loss peak. Heating to even higher temperature does not lead to discernible exo-/endo-thermic peaks or weight loss either.

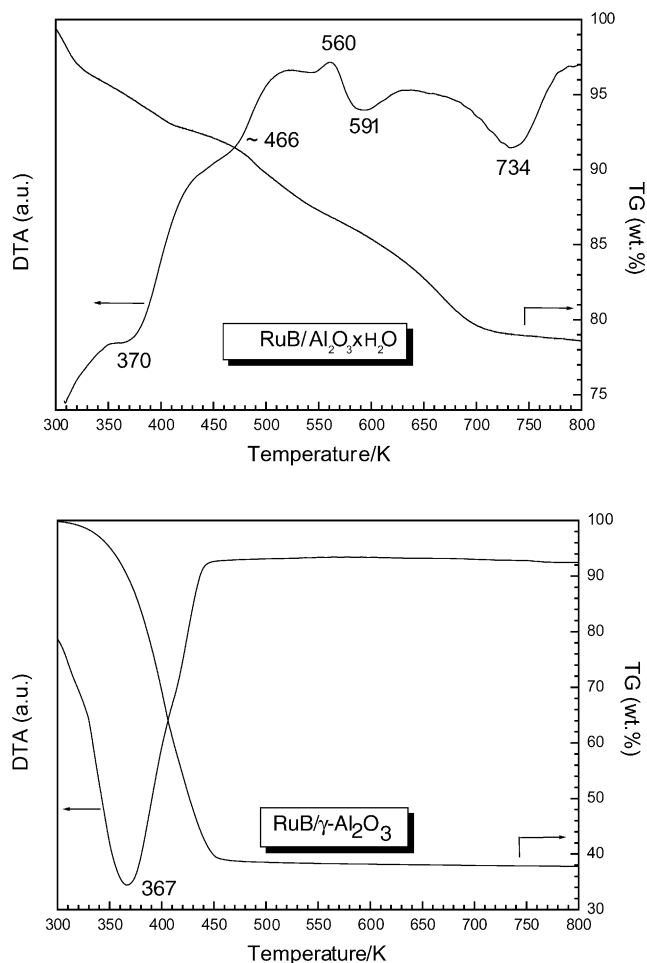The dimension of the catalyst particles of the colloidal RuB/$Al_2O_3 \cdot x$H$_2$O catalyst was measured by the dynamic light scattering method. It is found that the most probable particle size was found ca. 150 nm with a sole size distribution ranging from 40 to 375 nm, and the mean particle size was 200 nm. Fig. 3a shows the TEM image of the RuB/$Al_2O_3 \cdot x$H$_2$O catalyst which reveals further details on the morphology of the catalyst. The large gray flakes in this figure are crystallized aluminum hydroxide according to TG/DTA and additional TEM analysis on the catalyst precursor before reduction by KBH$_4$. The black particles homogeneously dispersed on the flakes with diameter of ca. 3.6 nm are RuB alloys based on EDX. In contrast, the RuB particles in the RuB/γ-Al_2O_3 catalyst are much larger, with diameter
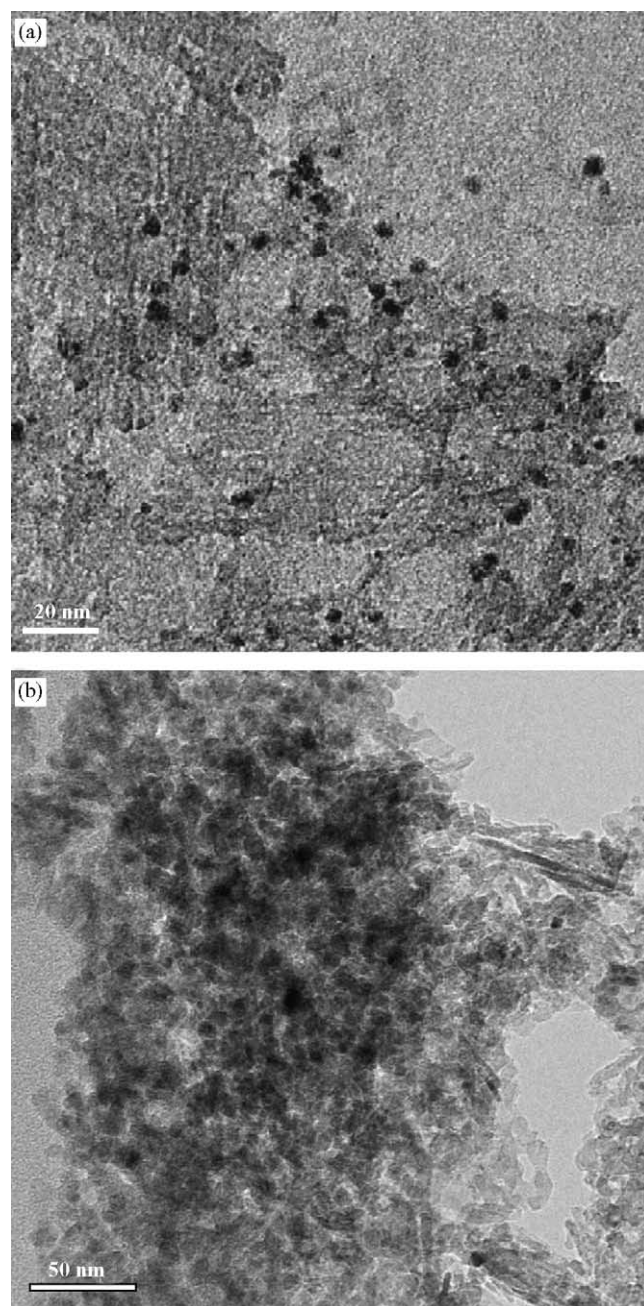

Fig. 2. The TG/DTA curves of (a) RuB/$Al_2O_3 \cdot x$H$_2$O and (b) RuB/γ-Al_2O_3 catalysts.

Fig. 3. TEM images of (a) RuB/$Al_2O_3 \cdot x$H$_2$O and (b) RuB/γ-Al_2O_3 catalysts.

of ca. 10 nm, and somewhat agglomerated as illustrated in Fig. 3b. These results are in good agreement with the XRD profiles shown in Fig. 1, in which no diffraction peak of RuB is observed for the RuB/Al$_2$O$_3$·xH$_2$O catalyst, whereas it is readily visible at 2θ of 43.1° for the RuB/γ-Al$_2$O$_3$ catalyst.

3.2. Catalytic performance in selective hydrogenation of benzene

Selective hydrogenation of benzene over the RuB/Al$_2$O$_3$·xH$_2$O catalyst has been carried out under the reaction conditions specified in the experimental part with the addition of an optimized amount of zinc sulfate of 4.0 g. Fig. 4a illustrates the evolutions of benzene, cyclohexene and cyclohexane during the hydrogenation process over the RuB/Al$_2$O$_3$·xH$_2$O catalyst. Both the conversion of benzene and the concentration of cyclohexane increased monotonously with reaction time. Moreover, the

(a)

(b)
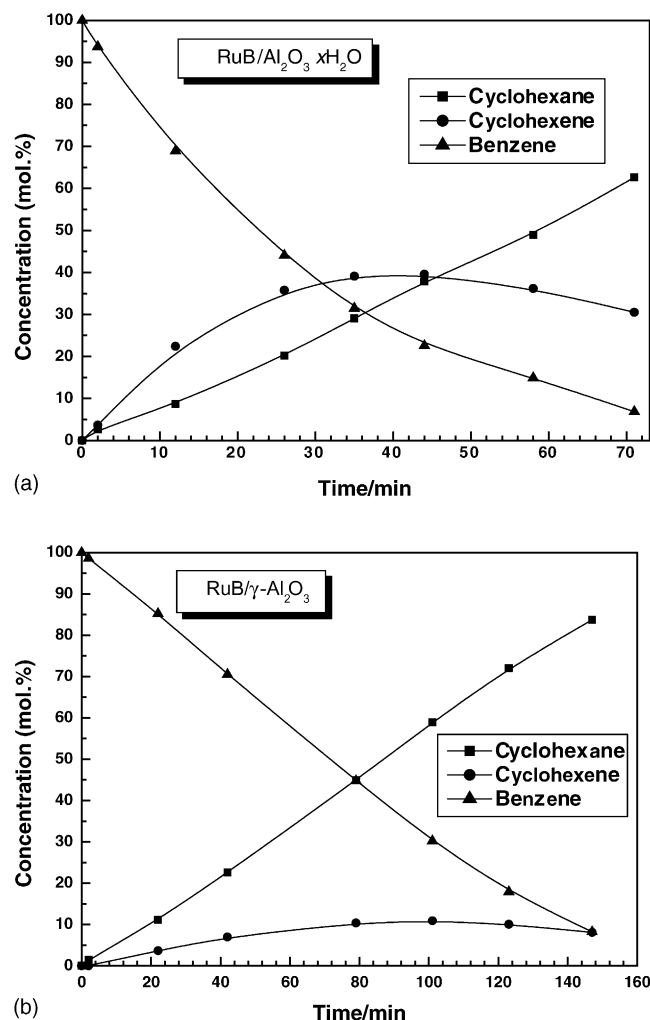
Fig. 4. The courses of benzene hydrogenation over (a) RuB/Al$_2$O$_3$·xH$_2$O and (b) RuB/γ-Al$_2$O$_3$ catalysts. Reaction conditions: 1.0 g of catalyst; 50 ml of benzene; 100 ml of water; reaction temperature 418 K; hydrogen pressure 4.28 MPa; stirring rate 1000 rpm.

concentration of cyclohexene increased much faster than that of cyclohexane at the beginning of the reaction, and reached a maximum of 39.6 mol% at benzene conversion of 77.4 mol% with reaction time of about 35 min. The cyclohexene yield then declined gradually following the known behavior of a consecutive reaction.

Fig. 4b gives the benzene hydrogenation process over the RuB/γ-Al$_2$O$_3$ catalyst for comparison. Note that for different catalyst the amount of zinc sulfate for attaining the highest yield of cyclohexene is different. For the RuB/γ-Al$_2$O$_3$ catalyst, the optimum amount of zinc sulfate was found to be 2.0 g. It is found that during the initial stage of the reaction, the growth of cyclohexane was much faster than that of cyclohexene, signifying the poor selectivity to cyclohexene over the RuB/γ-Al$_2$O$_3$ catalyst. The maximum yield of cyclohexene is only 10.9 mol% at benzene conversion of 58.9 mol% with reaction time of about 100 min.

Before comparing the selectivities over these catalysts, Carberry number (Ca) and Wheeler-Weisz number ($\eta\varphi^2$) were calculated according to Refs. [4,35], as the extent of mass-transfer limitations affects the selectivity towards cyclohexene [4]. It is assumed that a value of Ca smaller than 0.05 indicates that diffusion retardation by external mass transport may be neglected, whereas a value of $\eta\varphi^2$ smaller than 0.1 means that pore limitation is negligible [4]. Here the values of Ca and $\eta\varphi^2$ were estimated to be $\sim$1.7 × 10^{-11} and 3.4 × 10^{-5}, respectively, for the RuB/Al$_2$O$_3$·xH$_2$O catalyst, and $\sim$3.5 × 10^{-7} and 1, respectively, for the RuB/γ-Al$_2$O$_3$ catalyst. Thus the reaction over the RuB/Al$_2$O$_3$·xH$_2$O catalyst was always under kinetic control, while the inner particle diffusion controlled the reaction over the RuB/γ-Al$_2$O$_3$ catalyst. Although mass transfer limitations are important for obtaining a high selectivity at high conversion [4], the selectivity over the RuB/γ-Al$_2$O$_3$ catalyst was still inferior to that over the RuB/Al$_2$O$_3$·xH$_2$O catalyst, demonstrating that the RuB/γ-Al$_2$O$_3$ catalyst is intrinsically less selective than the RuB/Al$_2$O$_3$·xH$_2$O catalyst in benzene hydrogenation to cyclohexene.

The better activity of the RuB/Al$_2$O$_3$·xH$_2$O catalyst as compared to that of the RuB/γ-Al$_2$O$_3$ catalyst can be attributed to the higher dispersion of much smaller RuB particles on the RuB/Al$_2$O$_3$·xH$_2$O catalyst based on the XRD and TEM results, exposing more active sites for benzene hydrogenation. However, the dispersion and size of the ruthenium particles are found irrelevant to the selectivity in benzene selective hydrogenation [10,35]. Here, we tentatively attribute the superior selectivity towards cyclohexene over the RuB/Al$_2$O$_3$·xH$_2$O catalyst to a higher content of structural water and surface hydroxyl groups, which are expected to enhance greatly the hydrophilicity of the catalyst. Fig. 2a shows that for the RuB/Al$_2$O$_3$·xH$_2$O catalyst, in addition to the desorption of physisorbed water, there is continuous weight loss at higher temperatures. A simple analysis estimates that about 13.7 wt.% of structural water and hydroxyl groups exist in the RuB/Al$_2$O$_3$·xH$_2$O catalyst. Such structural water and hydroxyl groups may effectively

stabilize the water layer on the catalyst surface by hydrogen bonding, which is crucial for a high yield of cyclohexene [10]. In contrast, although γ-Al$_2$O$_3$ is known to have residual hydroxyl groups, the amount is marginal as confirmed by the present TG/DTA results showing that there is no significant weight loss after the desorption of physisorbed water.

It is worthy to note that tuning of hydrophilicity has become a common practice in heterogeneous catalysis to tailor the catalytic behavior of a catalyst. Besides selective hydrogenation of benzene to cyclohexene, it has been reported that the hydro-philic/phobic character of the catalyst has a marked effect on other industrially important processes including selective oxidation of olefins and alcohols [36,37], degradation of organic contaminants [38], hydrodehalogenation of chlorinated hydrocarbons [39], and hydroxylation of benzene [40]. Such character does not necessarily influence the nature of the active sites; however, it modifies the nano-environment around the active sites, which alters the effective local concentration of the reactants [41], e.g. cyclohexene and hydrogen in the present case. Aside from preparing the ruthenium catalyst on hydrophilic colloidal support, direct covering or "decoration" of the active sites by patches of hydrophilic oxides (SMSI) [42] can be another promising way to enhance the selectivity to cyclohexene. Such experiments are in progress in our laboratory and preliminary result supports the validity of our assumption.

4. Conclusion

The colloidal RuB/Al$_2$O$_3$·xH$_2$O catalyst is more active and selective than the RuB/γ-Al$_2$O$_3$ catalyst in selective hydrogenation of benzene to cyclohexene. The higher dispersion of the much smaller amorphous RuB nanoparticles over the RuB/Al$_2$O$_3$·xH$_2$O catalyst can be responsible for the superior activity. The higher selectivity is attributed to the existence of more structural water and surface hydroxyl groups on the RuB/Al$_2$O$_3$·xH$_2$O catalyst, which improves the hydrophilicity of the catalyst and stabilizes the water film which is essential for selective hydrogenation of benzene.

Acknowledgments

References

[1] H. Ichihashi, H. Yoshioka, US Patent 4,575,572 (1988), To Sumitomo chem. Co. Ltd.

[2] H. Nagahara, M. Konishi, US Patent 4,734,536 (1988), To Asahi chem. Ind. Co. Ltd.

[3] F. Matsunaga, Eur. Patent 316,142 (1987), To Mitsui Petrochem. Ind., Ltd.

[4] C. Milone, G. Neri, A. Donato, M.G. Musolino, L. Mercadante, J. Catal. 159 (1996) 253.

[5] P.T. Suryawanshi, V.V. Mahajani, J. Chem. Tech. Biotechnol. 69 (1997) 154.

[6] M.A. Vannice, J. Catal. 37 (1975) 449.

[7] M. Boudart, Adv. Catal. 20 (1969) 153.

[8] C.U.I. Odenbrand, S.T. Lundin, J. Chem. Tech. Biotechnol. 30 (1980) 677.

[9] S.C. Hu, Y.W. Chen, J. Chem. Tech. Biotechnol. 76 (2001) 954.

[10] J. Struijk, A. d'Agremond, W.J.M. de Regt Lucas, J.J.F. Scholten, Appl. Catal. A 83 (1992) 263.

[11] H. Nagahara, M. Konishi, JP 6,388,139 (1988), To Asahi chem. Ind. Co. Ltd.

[12] M. Hronec, Z. Cvengrošová, M. Králik, G. Palma, B. Corain, J. Mol. Catal. A 105 (1996) 25.

[13] Á. Molnár, G.V. Smith, M. Bartók, Adv. Catal. 36 (1989) 329.

[14] J.F. Deng, Curr. Top. Catal. 2 (1999) 1.

[15] M.H. Qiao, S.H. Xie, W.L. Dai, J.F. Deng, Catal. Lett. 71 (2001) 187.

[16] B. Liu, M.H. Qiao, J.Q. Wang, K.N. Fan, Chem. Commun. (2002) 1236.

[17] Z. Liu, W.L. Dai, B. Liu, J.F. Deng, J. Catal. 187 (1999) 253.

[18] S.H. Xie, M.H. Qiao, H.X. Li, W.J. Wang, J.F. Deng, Appl. Catal. A 176 (1999) 129.

[19] Z. Liu, S.H. Xie, B. Liu, J.F. Deng, New J. Chem. 23 (1999) 1057.

[20] S.C. Hu, Y.W. Chen, Ind. Eng. Chem. Res. 40 (2001) 6099.

[21] S.C. Hu, Y.W. Chen, Ind. Eng. Chem. Res. 40 (2001) 3127.

[22] S. Niwa, F. Mizukami, S. Isoyama, T. Tsuchiya, K. Shimizu, S. Imai, J. Imamura, J. Chem. Tech. Biotechnol. 36 (1986) 236.

[23] S. Niwa, F. Mizukami, M. Kuno, K. Takeshita, H. Nakamura, T. Tsuchiya, K. Shimizu, J. Imamura, J. Mol. Catal. 34 (1986) 247.

[24] Y.G. He, M.H. Qiao, H.R. Hu, Y. Pei, H.X. Li, J.F. Deng, K.N. Fan, Mater. Lett. 56 (2002) 952.

[25] Y. Chen, Catal. Today 44 (1998) 3.

[26] PDFMaint Version 3.0, Powder Diffraction Database, Bruker Analytical X-ray Systems GmbH, 1997.

[27] T.L. Hong, H.T. Liu, C.T. Yeh, S.H. Chen, F.C. Sheu, L.J. Leu, C.I. Wang, Appl. Catal. A 158 (1997) 257.

[28] M.L. Guzmán-Castillo, X. Bokhimi, A. Toledo-Antonio, J. Salmones-Blásquez, F. Hernández-Beltrán, J. Phys. Chem. B 105 (2001) 2099.

[29] D.L. Cocke, E.D. Johnson, R.P. Merrill, Catal. Rev. Sci. Eng. 26 (1984) 163.

[30] J.G. Li, X.D. Sun, Acta Mater. 48 (2000) 3103.

[31] P.A. Baldkar, J.E. Bailey, J. Mater. Sci. 11 (1976) 1794.

[32] D.L. Trimm, A. Stanislaus, Appl. Catal. 21 (1986) 215.

[33] N. Koga, T. Fukagawa, H. Tanaka, J. Therm. Anal. Cal. 64 (2001) 965.

[34] E. Morgado, Y.L. Lam, L.F. Nazar, J. Colloid Interface Sci. 188 (1997) 257.

[35] L. Ronchin, L. Toniolo, React. Kinet. Catal. Lett. 78 (2003) 281.

[36] A. Corma, P. Esteve, A. Martinez, J. Catal. 161 (1996) 11.

[37] Y. Deng, M.F. Maier, J. Catal. 199 (2001) 115.

[38] G. Centi, S. Perathoner, G. Romeo, Stud. Surf. Sci. Catal. 135 (2001) 181.

[39] C. Schüth, S. Disser, F. Schüth, M. Reinhard, Appl. Catal. B 28 (2000) 147.

[40] J. He, Z.Y. Guo, H. Ma, D.G. Evans, X. Duan, J. Catal. 212 (2002) 22.

[41] G. Centi, S. Perathoner, Catal. Today 79 (2003) 3.

[42] G.L. Haller, J. Catal. 216 (2003) 12.